

## Evidence for a first-order transition from monoclinic $\alpha$ to monoclinic $\beta$ phase in BiFeO<sub>3</sub> thin films

H. Toupet,<sup>1</sup> F. Le Marrec,<sup>1,\*</sup> C. Lichtensteiger,<sup>2</sup> B. Dkhil,<sup>3</sup> and M. G. Karkut<sup>1</sup>

<sup>1</sup>Laboratoire de Physique de la Matière Condensée, Université de Picardie Jules Verne, 80039 Amiens, France

<sup>2</sup>Département de Physique de la Matière Condensée, Université de Genève, CH-1211 Genève 4, Switzerland

<sup>3</sup>Laboratoire Structures, Propriétés et Modélisation des Solides, CNRS-UMR8580, Ecole Centrale Paris, 92295 Châtenay-Malabry Cedex, France

(Received 15 July 2009; revised manuscript received 30 July 2009; published 5 April 2010)

We report a temperature-dependent high-resolution x-ray diffraction investigation of 200-nm epitaxial BiFeO<sub>3</sub> thin films grown on (001) SrTiO<sub>3</sub>. We find that BiFeO<sub>3</sub> undergoes two high-temperature transitions: a first-order  $\alpha$ - $\beta$  phase transition between 745 and 780 °C and a more diffuse transition toward the  $\gamma$  phase at 860 °C. Reciprocal space maps reveal that thin films remain monoclinic crossing the  $\alpha$ - $\beta$  phase transition. Linear extrapolation of the in-plane lattice parameters to higher temperatures appears to rule out cubic symmetry for the  $\gamma$  phase.

DOI: 10.1103/PhysRevB.81.140101

PACS number(s): 68.55.-a, 61.05.cp, 77.55.-g, 77.80.B-

Among the single-phase multiferroics, BiFeO<sub>3</sub> (BFO) is the most studied<sup>1</sup> since it possesses a high ferroelectric Curie temperature  $T_C$  [810–850 °C (Refs. 2–5)] and a high antiferromagnetic Néel temperature  $T_N$  [370 °C (Ref. 6)]. At room temperature, bulk BFO crystallizes in a rhombohedrally distorted perovskite structure, called  $\alpha$  phase, with space group  $R3c$  and lattice parameters  $a=3.96$  Å and  $\alpha=89.4^\circ$ .<sup>7</sup> The transition from the ferroelectric  $\alpha$  phase to the paraelectric  $\beta$  phase is accompanied by an abrupt volume contraction that is indicative of a first-order transition. Despite extensive studies, the symmetry of this paraelectric phase is still subject of debate: rhombohedral,<sup>8</sup> monoclinic,<sup>9</sup> cubic,<sup>10</sup> and orthorhombic symmetries have been recently proposed<sup>4,5</sup> for the  $\beta$  phase. Part of the discrepancy concerning the symmetry may be attributed to difficulties in preparing high-quality single phase material since at high temperature the secondary phase Bi<sub>2</sub>Fe<sub>4</sub>O<sub>9</sub> is in thermodynamic-kinetic competition with BFO.<sup>11</sup> The  $\beta$ -phase symmetry is also not corroborated by first-principles calculations of Kornev *et al.*<sup>12</sup> since they predict that bulk BFO above  $T_C$  is tetragonal. Moreover, they expect a transition to a cubic  $\gamma$  phase at 1167 °C. But due to the instability of BFO in air at very high temperature, experimental evidence for this transition is scarce. To our knowledge, only Palai *et al.*<sup>4</sup> have reported that bulk BFO undergoes an orthorhombic-cubic  $\beta$ - $\gamma$  phase transition at 925 °C which coincides with an insulator-metal transition.

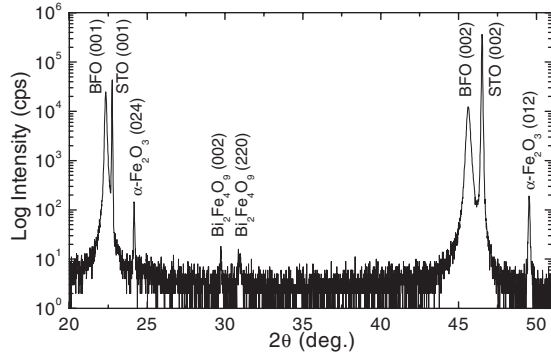
Most studies dealing with phase transitions in BFO take place on bulk samples while surprisingly few reports on thin films are available. The first phase diagram for BFO thin films, relying mainly on Raman spectroscopy, has established that the sequence of phases  $\alpha$ - $\beta$ - $\gamma$  for BFO thin films deposited on SrTiO<sub>3</sub> buffered with SrRuO<sub>3</sub> is monoclinic-orthorhombic-cubic.<sup>4</sup> The monoclinic structure observed at room temperature as well as its change from monoclinic to tetragonal when the thickness decreases have been extensively investigated.<sup>13–16</sup> This thickness dependence of the structure is ascribed to a competition between the rhombohedral distortion of bulk BFO and the epitaxial compressive strain imposed by the cubic substrate. Concern-

ing the  $\beta$  and  $\gamma$  phases, no other study to date confirms both the existence and the symmetry of these high temperature phases in thin films. In this paper, we provide x-ray diffraction evidence for the occurrence of two phase transitions at high temperature for epitaxial BFO thin films. We demonstrate the first-order nature of the  $\alpha$ - $\beta$  phase transition as well as the monoclinic symmetry of the  $\beta$  phase.

200-nm-thick BFO films were grown on (001) SrTiO<sub>3</sub> (STO) substrates using pulsed laser deposition with a KrF excimer laser ( $\lambda=248$  nm). For this study, films were deposited under 0.1-mbar oxygen pressure at a substrate temperature of 650 °C and subsequently *ex situ* anneals were performed at 850 °C. As reported elsewhere,<sup>17</sup> these specific growth conditions allow us to produce stable samples up to 900 °C which are required to study these phase transitions. Room temperature  $\theta$ - $2\theta$  x-ray diffractometry (XRD) was performed on a two-circle Siemens D5000 diffractometer whereas the temperature-dependent measurements were carried out on a high-precision diffractometer using Cu  $K\alpha$  radiation emitted from a 18 kW rotating anode. This in-house designed goniometer permits accurate determination of the out-of-plane lattice parameters up to 900 °C. The thin-film structure has been investigated by reciprocal space mapping (RSM) around (H0L) and (HHL) reflections using a high-resolution Philips “X’pert” diffractometer. It is equipped with PIXcel, a one-dimensional detector which significantly shortens the acquisition time compared to a standard detector reducing the danger of BFO decomposition at high temperatures.<sup>4</sup>

Figure 1 displays a typical room-temperature diffractogram of a BFO thin film. We observe intense BFO(001) reflections suggesting a good crystalline quality of the BFO phase. This is confirmed by the full width at half maximum (FWHM) of 0.23° for the BFO(001) rocking curve which is close to the substrate value of 0.15°. We also detect weak peaks corresponding to  $\alpha$ -Fe<sub>2</sub>O<sub>3</sub> and Bi<sub>2</sub>Fe<sub>4</sub>O<sub>9</sub> phases. However, these secondary phase reflections will not hinder the subsequent investigation of the BFO phase due to their large separation from the BFO peaks.

We present in Figs. 2(a) and 2(b) the XRD reciprocal


 FIG. 1.  $\theta$ - $2\theta$  diffractogram of a 200-nm BFO film on STO.

space maps around the (203) and the (223) reflections. The signal from the STO substrate is recorded at the same time as the film and acts as an internal unstrained standard. In Fig. 2(a), we observe a clear splitting of the BFO peak along the  $Q_Z$  direction. This splitting does not appear on the  $\theta$ - $2\theta$  scan of Fig. 1, contrary to what one expects for orthorhombic or higher symmetry: that the number of peaks observed along the  $Q_Z$  direction for (203) must equal the number of peaks observed in the  $\theta$ - $2\theta$  diagram. In addition, the well-defined single peak detected for BFO on Fig. 1 is exactly equal to the  $Q_Z$  average of the two (203) reflections and demonstrates that the symmetry for BFO film is lower than orthorhombic. In Fig. 2(b), the (223) reflection displays three peaks: one is

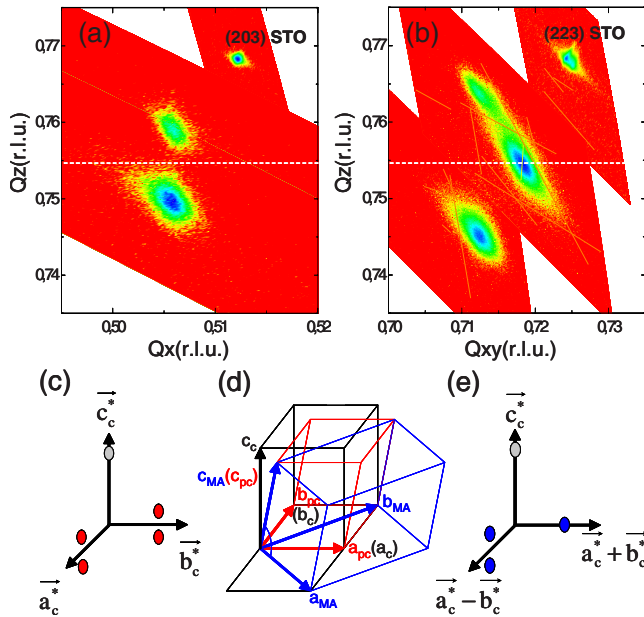


FIG. 2. (Color online) Room-temperature reciprocal space maps represented in reciprocal lattice units (r.l.u.) around the (a) (203) and (b) (223) reflections. Horizontal dotted lines indicate the out-of-plane parameter positions extracted from  $\theta$ - $2\theta$  scans. Schematics of domain configurations in the reciprocal space of (c) the primitive pseudocubic BFO unit cell and (e) the  $M_A$  monoclinic unit cell for which  $a_{MA}$  and  $b_{MA}$  lie along the pseudocubic  $[1\bar{1}0]$  and  $[110]$  directions, respectively. (d) Representation of the  $M_A$  monoclinic unit cell with respect to the pseudocubic and cubic unit cells. For reasons of clarity, we have put  $a_{MA} = a_c\sqrt{2} = a_{pc}\sqrt{2} = b_{MA}$ .

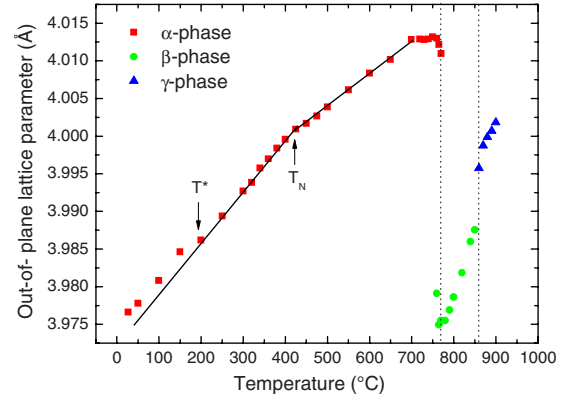


FIG. 3. (Color online) Evolution of the out-of-plane lattice parameter for BFO thin film with temperature. The solid lines emphasize the deviation in the slope around 200 °C ( $T^*$ ) and 425 °C ( $T_N$ ) and the vertical dotted lines indicate the structural phase transitions.

shifted up and the second is shifted down with respect to the central peak. This central peak coincides precisely with the out-of-plane lattice parameter deduced from the  $\theta$ - $2\theta$  scan of Fig. 1. The occurrence of two peaks around the (203) reflection along with the three peaks around the (223) provides clear evidence that the BFO film adopts a monoclinic structure of  $M_A$  type: the splitting around both the (023) (not shown here) and the (203) reflections is due to the four-variant domain structure of the primitive pseudocubic BFO unit cell [Fig. 2(c)] whereas the three peaks recorded around the (223) reflection come from the  $b_{MA}$  domain and the two  $a_{MA}$  domains of the monoclinic BFO unit cell [Fig. 2(e)]. The latter, as illustrated in Fig. 2(d), is doubled and rotated by 45° in the  $ab$  plane with respect to the pseudocubic cell. The monoclinic lattice parameters we extract from the (223) map and from the  $\theta$ - $2\theta$  scan are:  $a_{MA} = 5.615(3)$  Å,  $b_{MA} = 5.568(3)$  Å, (in-plane),  $c = 3.977(1)$  Å (out-of-plane), and  $\beta_{MA} = 89.25(10)^\circ$ . These values are consistent with the pseudocubic lattice parameters deduced from the (203) and (023) maps: we find for the in-plane pseudocubic parameters  $a_{pc} = b_{pc} = 3.953(2)$  Å, a value which fulfills the relation  $a_{pc} = b_{pc} = \sqrt{a_{MA}^2 + b_{MA}^2}/2$ . This in-plane parameter is not equal to that of the bulk ( $a = 3.96$  Å) meaning that the film is partially strained on the substrate.<sup>18</sup>

We now turn to the temperature-dependent measurements. Figure 3 shows the temperature evolution of the out-of-plane lattice parameter of the BFO film. Several heating and cooling cycles were performed and demonstrate the reproducibility of the x-ray measurements as well as the thermal stability of the BFO phase. The evolution, similar to that for BFO powder,<sup>4</sup> reveals four anomalies which cannot be ascribed to a substrate effect since the temperature dependence of the lattice parameter of STO (not shown here) is linear over the entire temperature range. These anomalies also cannot be assigned to strain relaxation nor to degradation of the BFO phase since these processes are irreversible. When the temperature increases, we first observe two anomalies, one at 200 °C and another at 425 °C. The latter corresponds to the Néel temperature  $T_N$  and contrary to the bulk, is not accompanied by an abrupt jump of lattice constants<sup>3,9</sup> but by a

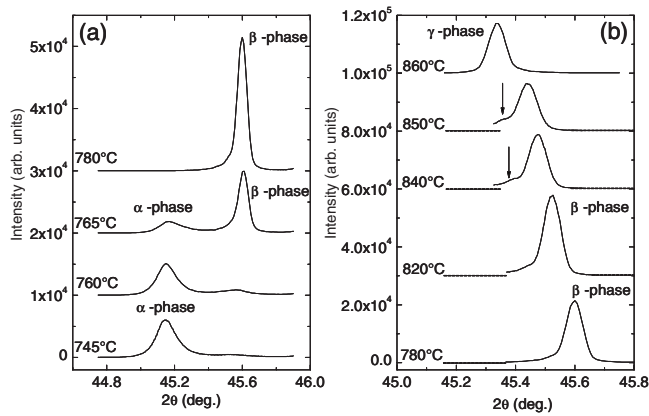


FIG. 4. X-ray diffraction patterns around the BFO(002) reflection as a function of temperature through (a) the  $\alpha$ - $\beta$  transition and (b)  $\beta$ - $\gamma$  transition. Arrows point out the emergence of the  $\gamma$  phase (see text). Dotted lines indicate the baseline for each scan in (b).

deviation in the slope. Thus, even in a thin-film, spin-lattice coupling can be detected. The anomaly at  $T^* = 200$  °C (Ref. 19) has already been observed in BFO powder and it has been proposed that the magnetic structure arranges itself continuously between  $T^*$  and  $T_N$ .<sup>9,20</sup> By increasing the temperature, two other striking anomalies are detected: the spectacular drop of the lattice parameter at 770 °C corresponds to the  $\alpha$ - $\beta$  phase transition while the sharp jump at 860 °C indicates the  $\beta$ - $\gamma$  phase transition.

To further explore the  $\alpha$ - $\beta$  phase transition, we display in Fig. 4(a) the  $\theta$ - $2\theta$  scans around the BFO(002) reflection in the vicinity of the drop. Below 745 °C and above 780 °C, only one peak is detected. However, the peak appears for quite distinct  $2\theta$  values and both its FWHM and its intensity are notably different, suggesting that a structural phase transition takes place. Additionally, between 745 and 780 °C, the diffraction patterns show two peaks coexisting with a striking inversion of peak intensity between 760 and 765 °C, similar to that reported for BFO powder.<sup>5</sup> These typical features argue that the  $\alpha$ - $\beta$  transition is first order. No thermal hysteresis is detected implying that if it exists, it must be less than 5 °C. It is worth noting that even if a first-order transition has been recently reported for Ca-doped BFO thin films,<sup>21</sup> such transitions, due to clamping on the substrate, rarely occur in perovskite epitaxial thin films. Furthermore, although we have no information about the polarization in the  $\beta$  phase, its similarities with the bulk suggest that the  $\alpha$ - $\beta$  transition also corresponds to the ferroelectric-paraelectric transition. Figure 4(b) shows the evolution of the BFO(002) reflection on going through the  $\beta$ - $\gamma$  transition. Between 820 and 840 °C, the intensity of the (002) reflection decreases significantly (30%) while a second weak peak appears at the  $2\theta$  position for the  $\gamma$  phase [see arrows in Fig. 4(b)]. However, the features of a first-order transition are markedly less pronounced than for the  $\alpha$ - $\beta$  phase transition, making problematic a conclusion concerning the order of the  $\beta$ - $\gamma$  transition.

Both the  $\alpha$ - $\beta$  and  $\beta$ - $\gamma$  transition temperatures take place about 60 °C lower whereas  $T_N$  occurs about 55 °C higher than in the bulk. Since we observe no change in the lattice

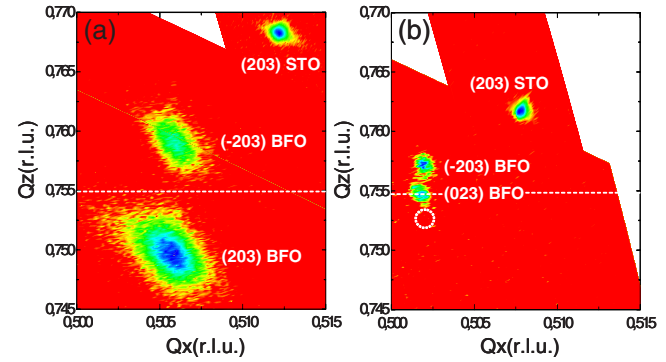


FIG. 5. (Color online) Reciprocal space maps represented in r.l.u. around the (203) reflection at (a) room temperature ( $\alpha$  phase) and (b) 780 °C ( $\beta$  phase). The RSM at room temperature is a slightly magnified image of RSM of Fig. 2(a). Horizontal dotted lines give the out-of-plane parameter positions extracted from  $\theta$ - $2\theta$  scans and the dotted circle indicate the missing (203) domain (see text).

parameter before and after these high  $T$  cycles, i.e., Fig. 3 remains the same, it does not seem that oxygen loss is a factor in these temperature shifts and that strain in the film is responsible. Recently, a downward shift in  $T_C$  with hydrostatic pressure<sup>22</sup> and an upward shift in  $T_N$  with chemical pressure<sup>23</sup> have been reported. This lends support to the strain origin of our results. Concerning the  $\alpha$ - $\beta$  transition, it is of interest to note that  $T_C$ , with respect to the bulk, decreases with strain in these epitaxial films. Indeed for classical compounds such as  $\text{PbTiO}_3$  and  $\text{BaTiO}_3$ , both experimental and theoretical studies have established that compressive strain tends to push  $T_C$  to higher temperatures.<sup>24,25</sup> This uncommon behavior observed for BFO emphasizes the complexity of the phase-transition mechanism involved in this perovskite material.

We now focus on the symmetry determination of the  $\beta$  phase. Figure 5 compares the RSM around the (203) Bragg reflection of the  $\alpha$  phase recorded at room temperature to the RSM of the  $\beta$  phase obtained just above  $T_C$  at 780 °C. Several remarkable features emerge. First, above  $T_C$ , the reflections arising from BFO are as sharp as that from the substrate which highlights the development of superior crystalline quality in the  $\beta$  phase. This result is also supported by Fig. 4 which shows at 780 °C an increase in the intensity and a decrease in the FWHM of the BFO(002) reflection. Second, we observe two reflections along the  $Q_Z$  direction. This splitting, as for the  $\alpha$  phase, cannot be assigned to an orthorhombic symmetry with two variants since the  $\theta$ - $2\theta$  diffractogram (see Fig. 4) reveals only a well-defined single peak. But contrary to what happens for the (203) reflection in the  $\alpha$  phase, the out-of-plane lattice parameter extracted from the  $\theta$ - $2\theta$  scan does not equal the  $Q_Z$  average of the two reflections [Fig. 5(a)] but instead exactly coincides with the lower reflection located at  $Q_Z = 0.7547$  r.l.u. [Fig. 5(b)]. This physically unreasonable situation can be resolved by evoking a missing (203) domain [Fig. 5(b)]. Such missing domain configurations are not unusual and can be induced by breaking the symmetry either by epitaxial strain, local inhomogeneities,<sup>13</sup> or by the use of vicinal substrates.<sup>26</sup>

Taking into consideration this missing domain, we conclude that the structure of the  $\beta$  phase is monoclinic. The persistence of the monoclinic symmetry in crossing the first-order  $\alpha$ - $\beta$  transition is of course not inconsistent with a paraelectric  $\beta$  phase. But contrary to the  $\alpha$  phase, the monoclinic unit cell for the  $\beta$  phase is primitive implying that  $a_M$  and  $b_M$  lie along the [100] and [010] directions of the pseudocubic unit cell. In addition, due to the domain structure of the primitive  $\beta$ -phase unit cell, we can simultaneously extract from the (203) RSM both the  $a_M$  and  $b_M$  in-plane lattice parameters. We obtain  $a_M=3.985(1)$  Å,  $b_M=3.986(1)$  Å,  $c_M=3.975(1)$  Å, (out-of-plane),  $\beta_M=89.86(3)^\circ$ .

Now, from the in-plane values extracted from the (203) RSM both at room temperature (i.e.,  $a_{pc}=3.953$  Å) and at 780 °C, we calculate the slope of the thermal expansion for the BFO film to be, within experimental accuracy, equal to that of the substrate (i.e.,  $4.3 \times 10^{-5}$  K<sup>-1</sup>.Å). This suggests, as previously reported for Pb(Zr<sub>0.2</sub>Ti<sub>0.8</sub>)O<sub>3</sub>,<sup>27</sup> that the film is firmly clamped on an effective substrate and the crossing of the strong  $\alpha$ - $\beta$  first-order transition occurs without modifying the dislocation density. Due to the limitation of the high-temperature stage used, no study of the  $\gamma$  phase by RSM was able to be performed. Nevertheless, by assuming that the film continues to follow the thermal expansion of the substrate,

we extrapolate an in-plane parameter for the BFO film of  $a=3.992$  Å just above the  $\beta$ - $\gamma$  phase transition at  $T=870$  °C. This linear extrapolation seems to rule out cubic symmetry of the  $\gamma$  phase since the out-of-plane parameter, determined from the  $\theta$ - $2\theta$  scan at the same temperature, is  $c=3.999$  Å.

In conclusion, we have provided x-ray diffraction evidence that epitaxial BFO thin films undergo two high-temperature transitions. Between 745 and 780 °C, a textbook case first-order  $\alpha$ - $\beta$  phase transition takes place without modification of the dislocation density. On going through this transition, the films remain monoclinic with however a noticeable change: the  $\alpha$  phase is doubled and rotated by 45° in the  $ab$  plane while the  $\beta$  phase is primitive without rotation. By increasing further the temperature, a sharp transition toward a noncubic  $\gamma$  phase occurs at 860 °C. Our results also suggest that the increase in  $T_N$  and the decrease of  $T_C$  with respect to bulk BFO are due to strain in the film.

We wish to thank J. F. Scott and P.-E. Janolin for illuminating discussions. This work was partially supported by the European 6th Framework STREP: “MULTICERAL” (Grant No. FP-6-NMP-CT-2006-032616).

\*francoise.lemarrec@u-picardie.fr

- <sup>1</sup>G. Catalan and J. F. Scott, *Adv. Mater.* **21**, 2463 (2009).
- <sup>2</sup>G. Smolenskii, V. Isupov, A. Agranovskaya, and N. Krainik, *Sov. Phys. Solid State* **2**, 2651 (1961).
- <sup>3</sup>J. D. Bucci, B. K. Robertson, and W. J. James, *J. Appl. Crystallogr.* **5**, 187 (1972).
- <sup>4</sup>R. Palai, R. S. Katiyar, H. Schmid, P. Tissot, S. J. Clark, J. Robertson, S. A. T. Redfern, G. Catalan, and J. F. Scott, *Phys. Rev. B* **77**, 014110 (2008).
- <sup>5</sup>D. C. Arnold, K. S. Knight, F. D. Morrison, and P. Lightfoot, *Phys. Rev. Lett.* **102**, 027602 (2009).
- <sup>6</sup>P. Fischer, M. Polomska, I. Sosnowska, and M. Szymanski, *J. Phys. C* **13**, 1931 (1980).
- <sup>7</sup>F. Kubel and H. Schmid, *Acta Crystallogr., Sect. B: Struct. Sci.* **46**, 698 (1990).
- <sup>8</sup>S. M. Selbach, T. Tybell, M.-A. Einarsrud, and T. Grande, *Adv. Mater.* **20**, 3692 (2008).
- <sup>9</sup>R. Haumont, I. A. Kornev, S. Lisenkov, L. Bellaiche, J. Kreisel, and B. Dkhil, *Phys. Rev. B* **78**, 134108 (2008).
- <sup>10</sup>R. Haumont, J. Kreisel, P. Bouvier, and F. Hippert, *Phys. Rev. B* **73**, 132101 (2006).
- <sup>11</sup>M. Valant, A.-K. Axelsson, and N. Alford, *Chem. Mater.* **19**, 5431 (2007).
- <sup>12</sup>I. A. Kornev, S. Lisenkov, R. Haumont, B. Dkhil, and L. Bellaiche, *Phys. Rev. Lett.* **99**, 227602 (2007).
- <sup>13</sup>G. Xu, H. Hiraka, G. Shirane, J. Li, J. Wang, and D. Viehland, *Appl. Phys. Lett.* **86**, 182905 (2005).
- <sup>14</sup>Y. H. Chu *et al.*, *Appl. Phys. Lett.* **90**, 252906 (2007).
- <sup>15</sup>D. S. Rana, K. Takahashi, K. R. Mavani, I. Kawayama, H. Murakami, M. Tonouchi, T. Yanagida, H. Tanaka, and T. Kawai, *Phys. Rev. B* **75**, 060405(R) (2007).
- <sup>16</sup>H. Béa, M. Bibes, S. Petit, J. Kreisel, and A. Barthélémy, *Philos. Mag. Lett.* **87**, 165 (2007).
- <sup>17</sup>H. Toupet, F. LeMarrec, J. Holc, M. Kosec, P. Vilarhino, and M. G. Karkut, *J. Magn. Magn. Mater.* **321**, 1702 (2009).
- <sup>18</sup>Fully strained high-quality epitaxial single-phase BFO films of up to 200 nm were also produced. But these samples systematically degrade when the temperature exceeds 600 °C, preventing the investigation of the phase transitions.
- <sup>19</sup>The degree of deviation in the slope at  $T^*$  is sample dependent.
- <sup>20</sup>M. Polomska, W. Kaczmarek, and Z. Pajak, *Phys. Status Solidi A* **23**, 567 (1974).
- <sup>21</sup>C.-H. Yang *et al.*, *Nature Mater.* **8**, 485 (2009).
- <sup>22</sup>S. Redfern, J. Walsh, S. Clark, G. Catalan, and J. Scott, [arXiv:0901.3748](https://arxiv.org/abs/0901.3748) (unpublished).
- <sup>23</sup>G. Catalan, K. Sardar, N. S. Church, J. F. Scott, R. J. Harrison, and S. A. T. Redfern, *Phys. Rev. B* **79**, 212415 (2009).
- <sup>24</sup>N. A. Pertsev, A. G. Zembilgotov, and A. K. Tagantsev, *Phys. Rev. Lett.* **80**, 1988 (1998).
- <sup>25</sup>P.-E. Janolin, F. LeMarrec, J. Chevreul, and B. Dkhil, *Appl. Phys. Lett.* **90**, 192910 (2007).
- <sup>26</sup>Y. H. Chu, M. Cruz, C.-H. Yang, L. Martin, P.-L. Yang, J.-X. Zhang, K. Lee, P. Yu, L.-Q. Chen, and R. Ramesh, *Adv. Mater.* **19**, 2662 (2007).
- <sup>27</sup>S. Gariglio, N. Stucki, J.-M. Triscone, and G. Triscone, *Appl. Phys. Lett.* **90**, 202905 (2007).